V European Conference on Computational Fluid Dynamics
ECCOMAS CFD 2010
J. C. F. Pereira and A. Sequeira (Eds)
Lisbon, Portugal,14-17 June 2010

NUMERICAL SIMULATION OF AIRFLOW THROUGH SIMPLIFIED VOCAL TRACT GEOMETRIES RELEVANT TO SPEECH PRODUCTION: PRELIMINARY RESULTS

Annemie Van Hirtum[*,†], **Kazunori Nozaki**[†]

[*]GIPSA-lab, UMR CNRS 5216, Grenoble Universities, France
e-mail: annemie.vanhirtum@gipsa-lab.grenoble-inp.fr
[†]Osaka University, Japan

Key words: LES, simplified vocal tract geometries, upper airways, speech production

Abstract. *Airflow through the upper airways is a basic ingredient for human speech production. In real life, the airflow is subjected to complex initial and boundary conditions defined by upper airway geometry, tissue properties and airflow. In order to increase understanding, the current paper considers airflow through simplified geometries derived from 'in-vivo' rigid and steady upper airway configurations relevant to different articulation positions. The airflow is simulated using Large Eddy Simulation in order to take into account turbulence production. The Reynolds number is fixed to 4000 for all considered geometries.*

1 INTRODUCTION

Human speech production is most important for everyday communication. From a physical point of view human speech utterances result from a complex fluid-structure interaction in the upper airways. In general, simplified physical flow and mechanical models are favored due to the remarkably - considering the simplicity of the models - prediction of important physical quantities such as the minimum lung pressure required to produce sustained vowels, *e.g.* /a/ [13]. In addition, simplified models require a limited number of parameters which can be related to meaningful physiological quantities such as the minimum aperture at the glottis. Despite the mentioned advantages of a simplified model approach, a more accurate and detailed description is required when considering human fricative sound production, *e.g.* /s/, for which turbulent flow is known to be essential. Indeed, since pioneering work in the 1960 introducing aero-dynamic and aero-acoustic principles [3], the underlying mechanism of fricative sound production is generally described as *noise produced due to the interaction of a turbulent jet, issued from a constriction somewhere in the vocal tract, with a downstream wall or obstacle* [15, 17, 7, 8]. Consequently, the position and shape of articulators like tongue and teeth determine the generation and development of the jet as well as its downstream interaction with a wall or obstacle as is indeed observed on human speakers [9, 12]. It follows that experimental and simulation studies have been performed in order to characterise and quantify the influence of articulators position and shape on the sound produced [16, 11, 10]. Nevertheless, the mentioned studies focus on the acoustics of fricative noise production and not on the flow. Therefore, flow data providing a systematic characterisation issuing from configurations relevant to human fricative production, *i.e.* moderate Reynolds Re numbers covering the range $2000 < Re < 10^4$ [18] and low Mach Ma number, are few. Obviously, model validation would benefit from additional flow data providing quantitative information on the flow field as pointed out by among others [7] in the framework of fricative production. Recently, single sensor anemometry was used to characterise the spatial velocity distribution issued from an extended conical diffuser ($Re = 7350$) [19]. The data allowed to validate self-similar flow models of jet development. In addition, the influence of the initial mean and fluctuating flow profile on the jet development and so on the model parameters was pointed out. Variation of the initial flow profile was uniquely due to varying the extension length of a uniform tube downstream a diffuser. The extended diffuser with varying extension length represents a constriction between the tongue and the palatal plane *somewhere* in the vocal tract. As such, the study illustrates to which extent the articulation position is likely to determine the flow development. Different consonants articulation positions are schematically illustrated in Fig. 1. Although, in the mentioned

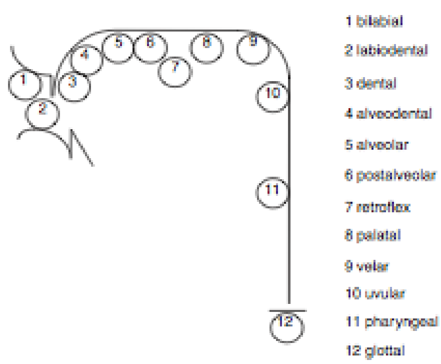

Figure 1: Schematic illustration of different consonant articulation positions in the vocal tract [14]. Variation of articulation position is further simplified in [19] as an extended conical diffuser with varying extension length.

study no obstacle, such as a tooth, was considered. In addition, obviously an extended diffuser is an extreme simplification of the vocal tract geometry. Important geometrical features, observed *in-vivo*, such as asymmetry, curvature and a sudden obstacle such as the teeth are neglected.

The objective of the current research is to contribute to the flow modeling of moderate bulk Reynolds number airflow within the range relevant to fricative production (∼4000) through simplified vocal tract geometries representing a constriction somewhere in the vocal tract as is the case during human articulation. In particular, the interaction of an

airflow with a downstream obstacle is searched.
The current simulation outcome of the mean and fluctuating part of the velocity fields - and related quantities such as vorticity - as well as their experimental validation is an important step towards fricative sound modeling.

2 Numerical flow simulation

2.1 Simplified geometry to accurate grid: degree and shape of constriction

Simplified vocal tract geometries representing different vocal tract portions during articulation are discretised. The spatial discretization of the flow domain was carried out using Gridgen (Pointwise, Inc.). A structured mesh was defined by using hexahedral finite elements with smaller elements near the walls to take into account the boundary layer effects whereas it was coarser in the body of the flow. Computational meshes are further refined in the constriction region and in the jet region. Geometries are designed to result in a mainly two-dimensional flow, so that the grid accuracy in the lateral dimension is chosen to be less accurate. The total grid size varied between 1.800.000 and 13.000.000 grid points depending on the geometry. In particular the degree and shape (sharp edges versus smooth edge, constriction length, obstacle position with respect to the jet center ...) of the minimum constriction is varied in order to study the influence of:

- changes in the geometrical shape of the constriction for a fixed minimum constriction corresponding to 8% of the upstream height
- the degree of constriction (4, 8, 16, 32 %) for a fixed geometrical shape

Obviously, the spatial dimension of the grids corresponding to the human upper airways is limited compared to major industrial mechanical applications (trains, fans, airplane wings). Consequently, the grid precision is very accurate (e.g. 300 grid points covering 1mm).

2.2 Inlet and boundary conditions

Boundary conditions were defined by specifying a uniform velocity profile at the channel entrance and a static pressure equal to 0 at the downstream domain exit. The inlet bulk Reynolds number is set to 4000 for all simulations. Moreover, the length of the channel upstream of the obstacle is chosen sufficiently high to obtain a fully developed parabolic velocity profile in the channel before the constriction. The no-slip wall condition was specified at all rigid wall boundaries.

2.3 Large Eddy Simulation

Three dimensional flow modeling was carried out using the Large-Eddy Simulation (LES) method for incompressible and isothermal flow implemented in Front Flow Blue

5 [6]. The subgrid-scale eddy-viscosity was computed using dynamic Smagorinskys turbulence model [5] for which the filter width is derived automatically from the mesh size. Second-order Crank-Nicolson scheme (implicit method) was used for the discretization of the momentum equation and a fractional-step method was used to compute the pressure field. The time step was varied between 10μs and 5ms depending on the geometry in order to ensure numerical stability. The inlet velocity was gradually increased during 0.1s after which the simulation was continued with a constant inlet velocity. The flow simulations were performed using NEC SX8 and SX9 vector supercomputers.

3 Numerical results: from teeth to glorttis-shaped nozzles

A schematic illustration of a two-dimensional teeth-shaped obstacle (bold lines) in relation to upper incisor morphological data [4, 1] is shown in Fig. 2. The geometry is further simplified and inserted in a rectangular channel so that a teeth-shaped nozzle is obtained with constriction degree 70%. Based on the resulting nozzle geometry some major geometrical and flow parameters derived from plane wall jet nomenclature [2] are determined in order to characterise the jet. This is motivated since the current problem is basically thought of as a two-layer shear flow consisting of an inner layer (similar to a boundary layer) and an outer layer (similar to a free shear layer) as is the case for a plane wall jet. The simulated velocity field inside the nozzle is illustrated in Fig. 3.

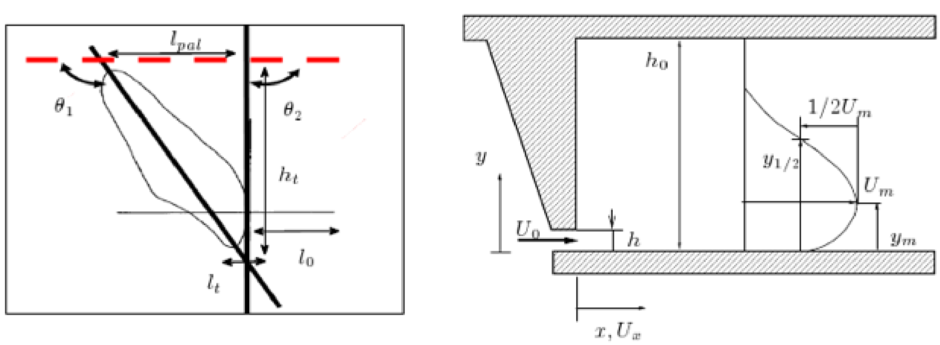

Figure 2: Two-dimensional teeth-shaped obstacle based on upper incisor morphological data and resulting teeth-shaped nozzle (70% constriction degree): transverse flow direction y, longitudinal flow component $U_x(x)$ in the main flow direction x indicated by a bold arrow, characteristic velocity at the constriction outlet U_0 at $x \approx 0$, aperture height h , channel height h_0, $y_m(x)$ distance from the wall up to the position of maximum flow velocity $U_m(x)$ in the transversal velocity profile, $y_{1/2}(x)$ distance from the wall up to the outer position where the velocity corresponds to $U_m/2(x)$.

Velocity profiles downstream the obstacle inside the nozzle are compared to hot wire anemometry data. In addition, the jet downstream of the nozzle is visualised by smoke visualisation and PIV measurements. Consequently, velocity data could be compared quantitatively in order to validate the simulated flow results. Validation is in particular important when aiming medical applications *e.g.* related to dental practice or speech

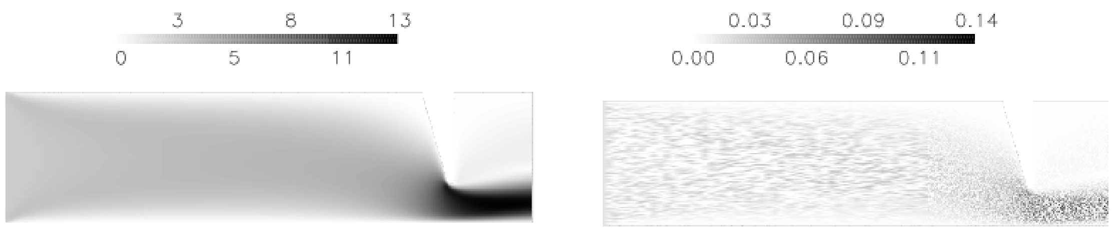

(a) mean (b) rms

Figure 3: Magnitude of mean and rms velocity for the teeth-shaped nozzle shown in Fig. 2.

therapy. An overview of the measured and simulated mean velocity profiles is shown in Fig. 4. From the comparison of the experimental and simulated flow features, it is seen

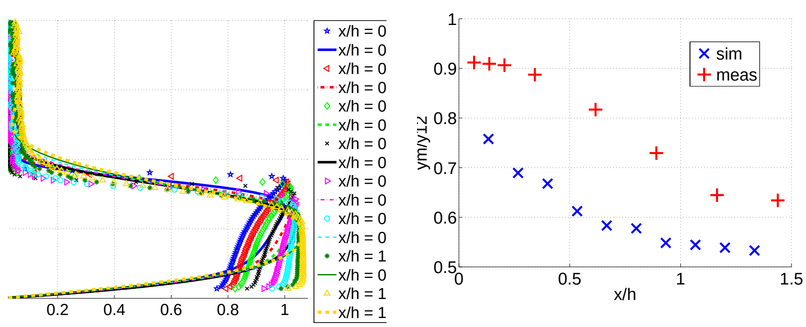

(a) mean (b) $y_m/y_{1/2}$

Figure 4: a) Measured (symbols) and simulated (lines) transverse mean velocity profiles for $0 < x/h < 1.5$. The magnitude of the profiles normalised with the characteristic velocity U_0 is plotted: $U/U_0(y/h)$ with h the aperture height. U_0 corresponds to the maximum of the initial transverse profile. b) Characteristic $y_m/y_{1/2}$ as illustrated in Fig. 2.

that the mean flow fields show the same general tendencies, but differ when considering the quantified features. The main common observations for the mean velocity include: 1) the position of maximum velocity y_m shifts towards the wall for increasing downstream position, 2) the maximum mean velocity U_m increases downstream the constriction, 3) the jet width is seen to decrease for increasing downstream position, 4) as does the ratio of the position of maximum velocity to the outer half width $y_m/y_{1/2}$. Nevertheless, some important differences are observed from the quantified mean velocity features with respect to the structure of the jet. The observed differences are the result of increased mean velocity and mean velocity gradients in the vicinity of the teeth edge, i.e. $y/h \approx 1$, for the experimental data compared to the simulated data. Both observations are important considering vorticity. The narrow peak near the teeth edge, observed on the measured mean velocity profiles, is accompanied with a narrow symmetrical peak in turbulence intensity up to 10%. The observed peak is absent in the simulated flow field, which is laminar in the near field downstream the constriction. Consequently, the observed differences in mean and turbulence intensities encourage further research in particular when sound production is of interest. It should be noted that although more accurate measurements can be performed, e.g. by using other measurement techniques, the observed differences largely exceed the uncertainty of the velocity measurements and are therefore significant.

It is evident that the considered 'teeth-shaped' geometry, although derived from morphological incisor data, does not account for variation of important morphological features such as location, orientation, shape, constriction degree, tissue properties, *etc.* In particular, different 'teeth' shapes and constriction degrees should be considered as exemplary illustrated in Fig. 5.

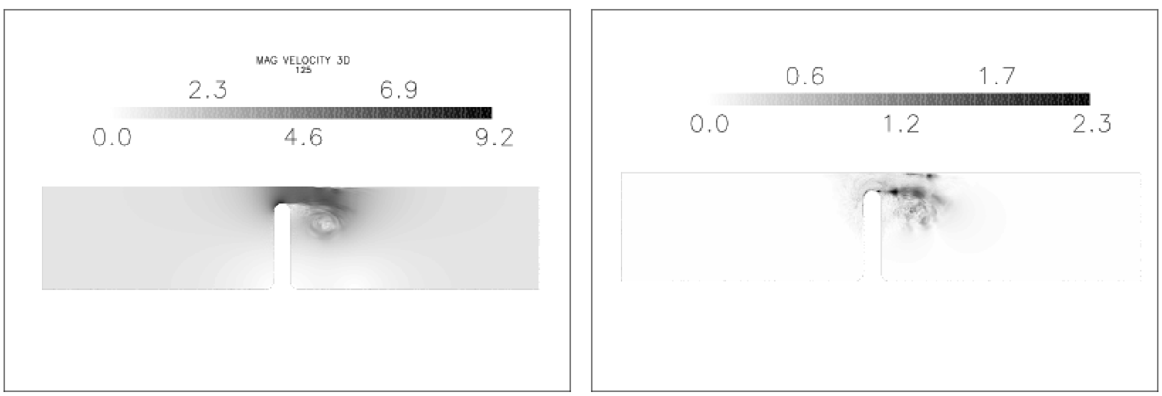

(a) mean (b) rms

Figure 5: Magnitude of mean and rms velocity for rounded teeth-shaped nozzle.

In addition, to sharp obstacles such as the teeth, important constriction can be situated somewhere in the upper airways between the glottis and the lips. The shape, degree and length of constriction can differ depending on the articulation condition and individual geometrical characteristics. The influence of shape is illustrated in Fig. 6 for a symmetric and antisymmetric constriction.

4 Conclusion

Data obtained from numerical simulations are assessed for different simple geometries inspired on different articulation positions for consonants, and fricatives in particular, along the vocal tract ranging from a symmetrical glottal constriction to a teeth-shaped

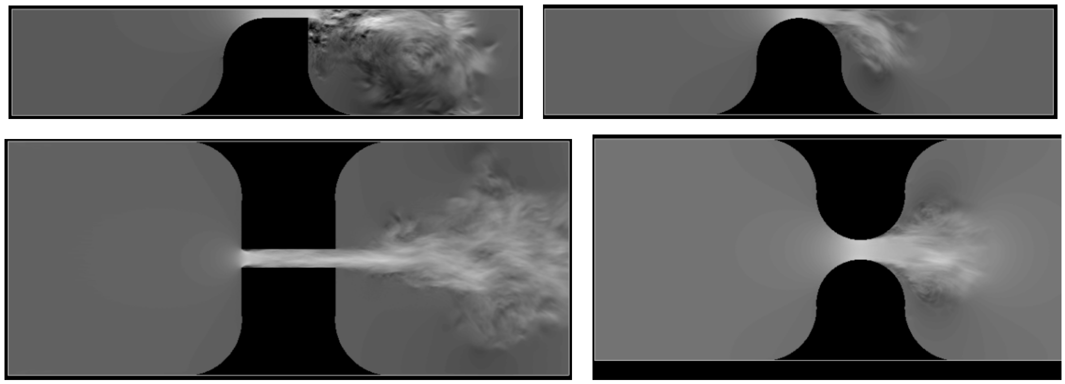

Figure 6: Magnitude of mean velocity for different constrictions.

obstacle. In particular, the influence of constriction degree, shape and length on the flow development is searched in order to increase understanding of the resulting flow features and quantities important for sound production such as vorticity, turbulence, *etc.* In addition, attention is given to the need to validate the simulation results towards experimental data.

Acknowledgements

Financial support of the petaflow ANR-JST project (CSD1-ANR-09-BLAN-0376-01) is gratefully acknowledged. A. Van Hirtum thanks the Japanese Society for the Promotion of Science (PE07072) for financial support.

REFERENCES

[1] E. Ellis and J.A. .McNamara. Cephalometric evaluation of incisor position. *The Angle Orthod*, pages 324–344, 1986.

[2] J. Eriksson, R. Karlsson, and J. Person. An experimental study of a two-dimensional plane turbulent wall jet. *Exp. Fluids.*, 20:50–60, 1998.

[3] G. Fant. *The acoustic theory of speech production*. Mouton, The Hague, 1960.

[4] C.D. Fredericks. A method for determining the maxillary incisor inclination. *Angle Orthod*, 44:341–345, 1974.

[5] M. Germano, U. Piomelli, P. Moin, and W. Cabot. A dynamic subgrid-scale eddy viscosity model. *Phys Fluids A*, 3:1760–1765, 1991.

[6] Y. Guo, C. Kato, Y. Yamade, and M. Uddin. Large Eddy simulation of several benchmark flows using finite element method. *JSFM*, 57:18–22, 2004.

[7] M. Howe and R. McGowan. Aeroacoustics of [s]. *Proc. R. Soc. A*, 461:1005–1028, 2005.

[8] M. Krane. Aeroacoustic production of low-frequency unvoiced speech sounds. *J. Acoust. Soc. Am.*, 118(1):410–427, 2005.

[9] S. Narayanan, A. Alwan, and K. Haker. An articulatory study of fricative consonants using magnetic resonance imaging. *J. Acoust. Soc. Am.*, 98:1325–1347, 1995.

[10] K. Nozaki, T. Akiyama, S. Shimojo, S. Maeda, and H. Tamagawa. Integration of computational fluid dynamics and computational aero acoustics on grid for dental applications. In *Proc. IEEE CBMS*, page 6, 2005.

[11] G. Ramsay. The influence of constriction geometry on sound generation in fricative consonants. In *Proc. Acoustics08*, pages 1–4, Paris, France, 2008.

[12] C. Runte, M. Lawerino, D. Dirksen, F. Bollmann, A. Lamprecht-Dinnesen, and E. Seifert. The influence of maxillary central incisor position in complete dentures on /s/ sound production. *The journal of prosthetic dentistry*, 85:485–495, 2001.

[13] N. Ruty, X. Pelorson, A. Van Hirtum, I. Lopez, and A. Hirschberg. An in-vitro setup to test the relevance and the accuracy of low-order vocal folds models. *J. Acoust. Soc. Am.*, 121(1):479–490, 2007.

[14] J. Schwartz, L. Boe, and C. Abry. *Linking Dispersion-Focalization Theory and the Maximum Utilization of the Available Distinctive Features Principle in a Perception-for-Action-Control Theory. In:Experimental Approaches to Phonology.* Oxford University Press, 2007.

[15] C. Shadle. *The acoustics of fricative consonants.* PhD thesis, Massachusetts Institute of Technology, 1985.

[16] C. Shadle. The effect of geometry on source mechanisms of fricative consonants. *J. Phonetics*, 19:409–424, 1991.

[17] D. Sinder. *Speech Synthesis Using an Aeroacoustic Fricative Model.* PhD thesis, 1999.

[18] K Stevens. *Acoustic Phonetics.* MIT Press, London, 1998.

[19] A. Van Hirtum, X. Grandchamp, and X. Pelorson. Moderate Reynolds number axisymmetric jet development downstream an extended conical diffuser: influence of extension length. *Eur. J. Mech - B/FLUIDS*, 28:753–760, 2009.